Eur. Phys. J. E **9**, 427–434 (2002)
DOI 10.1140/epje/i2002-10095-y

THE EUROPEAN PHYSICAL JOURNAL E

UV isomerisation in nematic elastomers as a route to photo-mechanical transducer

J. Cviklinski, A.R. Tajbakhsh, and E.M. Terentjev[a]

Cavendish Laboratory, University of Cambridge, Madingley Road, Cambridge CB3 0HE, UK

Received 12 August 2002 /
Published online: 28 January 2003 –

Abstract. The macroscopic shape of liquid-crystalline elastomers strongly depends on the order parameter of the mesogenic groups. This order can be manipulated if photo-isomerisable groups, *e.g.* containing N=N bonds, are introduced into the material. We have explored the large photo-mechanical response of such an azobenzene-containing nematic elastomer at different temperatures, using force and optical birefringence measurements, and focusing on fundamental aspects of population dynamics and the related speed and repeatability of the response. The characteristic time of "on" and "off" regimes strongly depends on temperature, but is generally found to be very long. We were able to verify that the macroscopic relaxation of the elastomer is determined by the nematic order dynamics and not, for instance, by the polymer network relaxation.

PACS. 83.80.Va Elastomeric polymers – 61.30.-v Liquid crystals – 82.50.Hp Processes caused by visible and UV light

1 Introduction

It has recently been demonstrated [1,2] that properly designed liquid-crystalline elastomers (LCE) can exhibit very strong photo-mechanical effects. Typical LCE are permanently crosslinked networks of polymer chains incorporating mesogenic groups either directly into the backbone or as side groups, attached end-on or side-on to a flexible backbone. Such materials, which have been synthetically available for a few years [3], couple the mobile anisotropic properties of liquid crystals to the rubber-elastic matrix; many novel and interesting physical effects arise from this association. For example, the mechanical shape of a monodomain nematic LCE [4] strongly depends on the underlying nematic order, which is a function of temperature. As the liquid-crystalline assembly undergoes the nematic-isotropic transition, it loses the associated anisotropy of polymer backbone chains induced by the coupling to nematic order. This leads to the macroscopic shape change of the sample, a uniaxial contraction, which can be utilised as a thermally driven artificial muscle [5]. The contraction can reach more than 300%, with a stress rising up to $\sim 100\,\mathrm{kPa}$, [6,7] and is theoretically well understood since the late '80s [8,9].

The nematic order parameter could be manipulated by means other than temperature, for example by applying an external stress or electric field, although the latter has been so far shown to have only a small effect. Another interesting way of affecting the nematic order is by introducing photo-isomerisable groups into the chemical structure, so that the mesogenic rod-like molecular shapes can be contorted by absorption of an appropriate photon. Several such groups are known in radiation chemistry, *e.g.* stilbenes or imines [10,11], but the most studied material in the context of liquid crystals is certainly azobenzene [12,13], Figure 1. As their N=N bond is in the equilibrium *trans* state, the mesogenic moieties are straight and rigid, and as such contribute to the formation of the overall nematic order. In the metastable *cis* state the N=N bond is strongly bent so that the molecular group no longer has the rod-like shape. Thus, the proportion of *cis* isomers

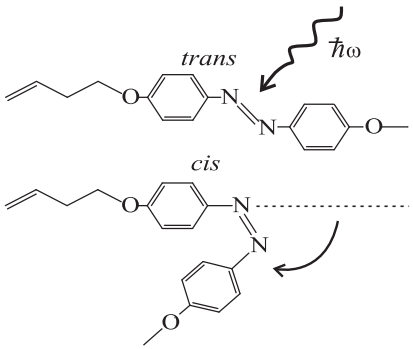

Fig. 1. The effect of azobenzene *trans*→*cis* isomerisation on the molecular shape.

[a] e-mail: emt1000@cus.cam.ac.uk

reduces the nematic order and shifts the clearing point to lower temperatures, as any other non-mesogenic impurity would. The resonant frequencies of radiation used to produce these molecular transformations are approximately the same in dense polymer systems as in dilute solutions [13]: 365 nm for *trans*→*cis* and 465 nm to achieve the back (*cis*→*trans*) reaction, which also occurs on heating. When azobenzene groups are incorporated into the polymer chains of a network crosslinked into a uniaxially aligned nematic elastomer[1], the photo-induced reduction of nematic order (fully analogous to heating) results in a uniaxial contraction of the sample, or an increase in force if the sample is mechanically restricted.

Such photo-mechanical effect in a monodomain nematic elastomer has been reported for the first time by Finkelmann *et al.* [1] and studied in some detail by Hogan *et al.* [2]. However, photo-induced mechanical actuation has been performed much earlier, using ordinary isotropic polymer networks [16,17], in which the required initial anisotropy has been induced by load. The magnitude of these effects was 10^2–10^3 times smaller, with strains of 0.15–0.25%, and was caused by mechanical contraction of (aligned) network crosslinks containing azobenzene groups. The large uniaxial contraction on irradiation of nematic rubbers is a much more spectacular effect with a different physical origin.

The main obstacle to turn this effect into a number of appealing applications is its rather slow dynamics [1,2]. On irradiation, the response was taking minutes, sometimes hours, to reach its saturation and it was similarly slow to relax. Could this be caused by a slow mechanical relaxation in the nematic elastomer, some time being necessary to change its conformation, or is it just the photo-isomerisation kinetics that is so slow? At first glance, the first option appears quite reasonable because it is indeed known that nematic elastomers are notoriously slow in their mechanical relaxation [18,19]. In addition, it is known that although the kinetics of *cis*→*trans* isomerisation in dilute solutions is very fast, in the range of milliseconds [20], the effect in dense polymer melts has always been reported to be slow too [14,15,17], suggesting the possible role of polymer dynamics.

To answer this fundamental question, and to try to validate more quantitatively the models of isomerisation kinetics, we have studied the photo-mechanical response of monodomain nematic rubber with azobenzene-containing mesogenic groups in end-on side chains (thus affecting the nematic ordering, but not having the direct mechanical effect of network crosslinks [1,17]). We measured the force exerted upon UV irradiation on the clamps restricting the sample length. Such a configuration requires no physical movement of chains in the network, as opposed to the measurements of changing length of a freely suspended sample [1,2], when the slow polymer relaxation could be a greater issue. We, however, found no increase in the speed of photo-mechanical response. The conclusion that the rate-limiting process is the photo-isomerisation itself has been further proven by the simultaneous measurement of the nematic order parameter, the dynamics of which exactly matched the mechanical response.

[1] One should also mention the important work on non-aligned nematic side-chain azopolymers [14,15].

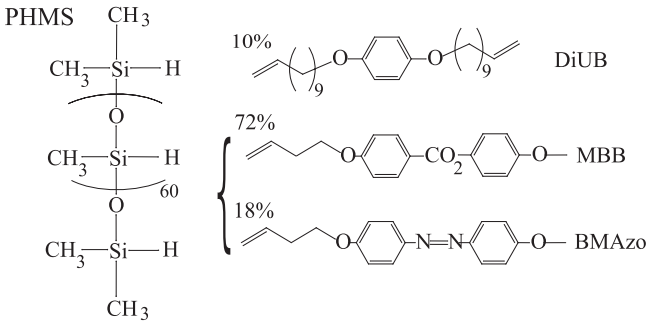

Fig. 2. The chemical structures of the compounds used in the present work, and their mol% concentrations.

This paper is organised as follows. The next section gives a very brief description of the material preparation, since we use the same (or very similar) materials as those studied in the pioneering works [1,2], as well as the details of experimental approach. Section 3 describes the photo-mechanical response in the "UV-on" and "UV-off" states, at different temperatures. Section 4 gives the results of the parallel measurement of the nematic order parameter and relates its magnitude to the simple linear model of population dynamics of photo-isomerisation. This data analysis confirms the validity of the linear model and identifies its key parameters. In the Conclusion we summarise the results and prospects.

2 Experimental

2.1 Preparation of nematic LCE

The starting materials and resultant aligned, monodomain nematic liquid-crystal elastomer were prepared in our laboratory. The procedure for making the side-chain polysiloxanes by reacting the terminal vinyl group in the mesogenic moiety with the Si-H bond of the polysiloxane chain, as well as the two-step crosslinking technique with a uniaxial stress applied after the first stage of crosslinking to produce and freeze the monodomain nematic alignment, has been developed over the years by Finkelmann *et al.* [4,21]. A number of minor modifications made to the original procedure are described in [2,7]. The azobenzene compounds were all synthesised according to standard literature techniques [22–24]. These compounds, and the final composition of the nematic elastomer, are given in Figure 2. This choice of components and concentrations was dictated by the results of [2], where the photo-mechanical response was maximised for this combination. We consciously avoided placing the azobenzene groups into network crosslinks, as in [1,2,17], in order to eliminate the direct mechanical coupling to the network: our purpose here is to study the effect induced purely by the changing nematic order.

The main mesogenic, rod-like units MBB[2] are known to produce a wide-range nematic phase and also reasonably stable under UV irradiation (a number of stray photo-chemical reactions could occur in such complex organic compounds). The photo-isomerisable rod-like groups were BMAzo[3]. Both these end-on side groups have a 4-carbon spacer, which induces a parallel orientation of the rods to the siloxane backbone resulting in a prolate chain anisotropy in the nematic phase, with its principal radii of gyration $R_{\parallel} > R_{\perp}$ [25]. The di-vinyl crosslinking agent is the flexible, non-mesogenic DiUB[4] which is known to have only a minor mechanical effect on the nematic network, preserving soft elasticity and allowing sharp near-critical evolution on phase transformation. The polymer backbone onto which all these compounds were grafted was polyhydromethylsiloxane (PHMS), containing approximately 60 SiH groups per chain, obtained from ACROS Chemicals. The polymer network was crosslinked *via* a hydrosilation reaction, in the presence of a commercial platinum catalyst COD, obtained from Wacker Chemie. The final composition of the elastomer is, per Si unit, 72% MBB, 18% BMAzo and 10% DiUB (the latter figure means that, on average, there are 9 mesogenic side groups between crosslinking points).

Phase sequences were established on a Perkin Elmer Pyris 1 differential scanning calorimeter, which was correlated with the critical temperature obtained by the thermal expansion measurements and optical microscopy between crossed polars. The permanently aligned monodomain networks were prepared by the two-step crosslinking reaction under load [4]. In the resulting elastomeric material a broad nematic liquid-crystalline phase was observed, between $T_{\rm ni} = 79$ °C and the glass transition at $T_{\rm g} \approx 0$ °C; optical microscopy, X-ray scattering and mechanical testing confirmed that this was indeed the nematic phase.

2.2 Mechanical measurements

Our mechanical setup is a custom-built device measuring the force exerted by the sample, and allowing to impose a fixed length and accurately maintain the temperature of the sample; see [7,18] for more detail. The accuracy of the force measurements is $\pm\, 4 \cdot 10^{-5}$ N ($\pm$ 0.4 mg).

The rectangular samples ($\sim$10×2.5×0.27 mm) were mounted with rigid clamps. The thermocouple was then placed behind the sample, as close as possible. As long as the temperature variations are slow, this enables us to measure the temperature of the sample. Of course, concerning the temperature measurements, the ideal would have been to imbed the thermocouple directly into the sample during crosslinking, but this would have affected both mechanical properties and the nematic order. As a compromise, we placed the thermocouple between the sample and the clamp during one of the experiments. No difference was found from the case with a thermocouple close behind the sample.

The UV radiation was produced by a Merck-4.L lamp (power 4 W) providing a narrow band at 365 ± 20 nm. The window of the thermally controlled compartment, allowing the passage of the radiation, was a single standard microscope slide, causing a 10% loss. The intensity of the radiation reaching the sample was 6 mW/cm^2 (measured by a calibrated photodiode) and kept constant during the experiments.

The sequence of a typical experiment was as follows:

- The mechanical history of the sample is first eliminated by annealing, to start all experiments from the same conditions. The unconstrained sample was heated to $\sim$ 120 °C and then cooled (slower than 0.3 °C/min) to the ambient temperature.
- The sample was clamped in the dynamometer. The temperature was then set to a value that will then be kept as constant as possible and the sample equilibrated at this temperature.
- The length of the sample was increased from the natural relaxed value to a marginally higher value. Thus the force exerted on the sample increased to a stable value above noise. The sample is equilibrated at this small extension.
- At last, the elastomer is exposed to UV radiation. The force increases with time and eventually reaches saturation. The force and the temperature of the sample are constantly logged on the computer.
- The source of UV radiations is switched off and the sample is screened from all light. The force decreases with time and, finally, both the force and the temperature reach the initial values, set before the UV irradiation.
- After final equilibration, the temperature of the sample was given a small variation ($\pm$2–3°) and the force variation logged in order to verify the underlying thermo-mechanical coefficient required in the subsequent data analysis.

The raw data for the force, transformed into stress by calibrating and dividing over the (constant) sample cross-section area, and the temperature readings were then used in the analysis of the process kinetics.

2.3 Birefringence measurements

The optical birefringence $\Delta n = n_{\parallel} - n_{\perp}$ is one of the main, and very accurate, measures of the degree of orientational order in liquid crystals. It was determined using the method based on measuring the lock-in phase difference θ between the split parts of polarised laser beam, one passing through the birefringent sample followed by the rotating analyser, the other through the beam chopper providing the reference frequency, see Figure 3. The phase difference between the two beams is measured by an integer number of periods, N, plus θ, and is related to Δn through equation (1), where λ is the wavelength of

[2] 4′-methoxyphenyl-4-(4″-buteneoxy)benzoate.
[3] [4-(4″-buteneoxy)-4′-methyloxy]azobenzene.
[4] di-1,4-(11-undeceneoxy)benzene.

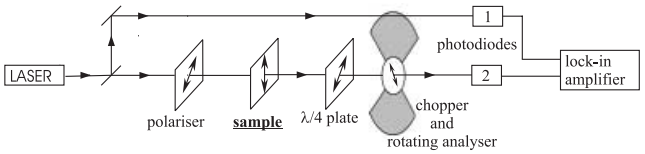

Fig. 3. Scheme of differential birefringence measurement, measuring the phase difference between the two beams, after [26]. The free beam (1) is chopped, giving the reference frequency to lock into; the phase lag of the beam (2) is proportional to the birefringence Δn.

the laser, d the thickness of the sample:

$$\Delta n = \frac{\lambda}{d}\left(N + \frac{\theta}{2\pi}\right) . \qquad (1)$$

The details of this fast and accurate method are described in [26]. In our experiments, we have continuously logged the values of Δn as a function of time, before, during and after UV irradiation. The kinetics of the nematic order change, directly reflecting the population dynamics of *cis* and *trans* azobenzene isomers, was then compared with that of the mechanical response.

3 Photo-mechanical response

As long as no radiation is applied, the local nematic order parameter Q is a function of temperature. If the monodomain texture is established in an elastomer, then the overall degree of director alignment has the same magnitude[5]. In this case the elastomer's natural length along the director is determined by this order parameter. Therefore, this natural length is very sensitive to temperature variations, see Figure 4(a). If, on the other hand, the sample shape is rigidly constrained, then instead a force is exerted on the clamps, Figure 4(b), which is in direct proportion to the internal strain due to the underlying changing natural length [7]. One can notice a difference between the two representations of this thermo-mechanical effect: the length of the freely suspended sample, proportional to the nematic order $Q(T)$, changes in an abrupt near-critical fashion near the $T_{\rm ni}$. In contrast, when the sample is rigidly clamped at room temperature (well below $T_{\rm ni}$), it will shorten its natural length on heating, thus generating an increasing uniaxial strain in the material; the stress response to this strain is registered by the dynamometer, Figure 4(b). So, as the sample approaches its phase transition, it finds itself under an increasing external uniaxial stress —as a result, the transition to isotropic phase near the $T_{\rm ni}$ occurs in a diffuse supercritical fashion.

This strong dependence on temperature has an adverse effect on our photo-mechanical measurements. Figure 5 shows an example set of raw data on irradiating a sample clamped in the dynamometer. As the sample, absorbing

[5] As opposed to, *e.g.*, polydomain nematic where the local order is Q, but globally the degree of director alignment is zero.

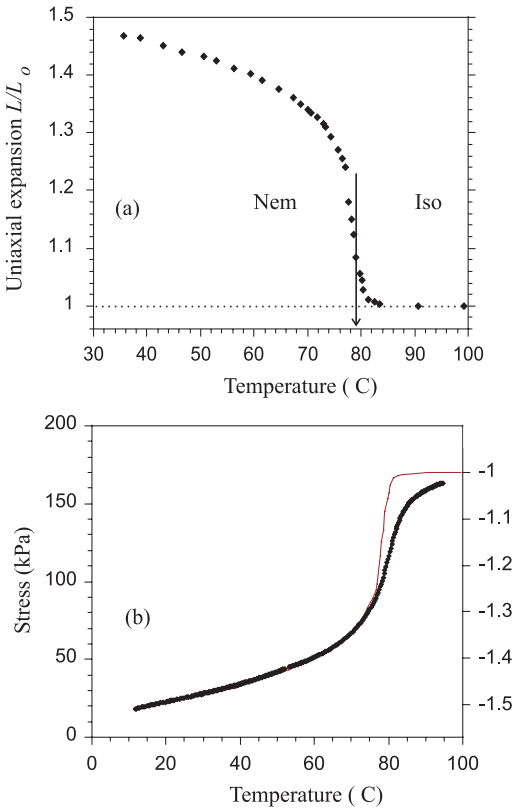

Fig. 4. Thermo-mechanical properties of the monodomain nematic elastomer. Plot (a) shows the equilibrium uniaxial expansion/contraction with temperature between the isotropic and the nematic phase below $T_{\rm ni} \approx 79$ °C. Plot (b) shows the stress arising in the elastomer when it is rigidly clamped at low temperature and not allowed to contract on heating. The thin solid line, right y-axis, shows the (negative of) strain data from (a), indicating the direct proportionality of the stress and strain at low temperatures and strong deviations near $T_{\rm ni}$.

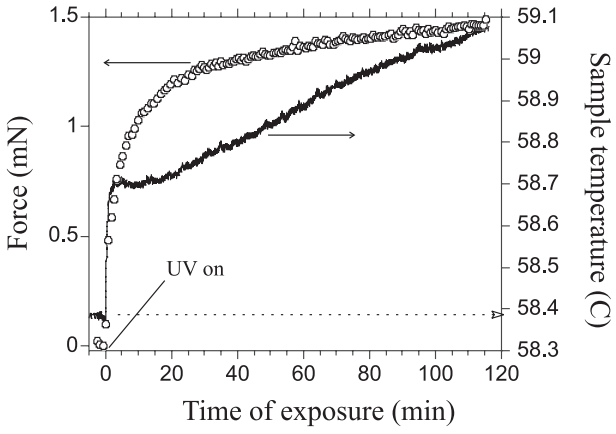

Fig. 5. The measured force (open circles, left y-axis) and the measured temperature variation on the sample (scatter line, right y-axis). The initial temperature of 58.4 °C is shown by the dotted line.

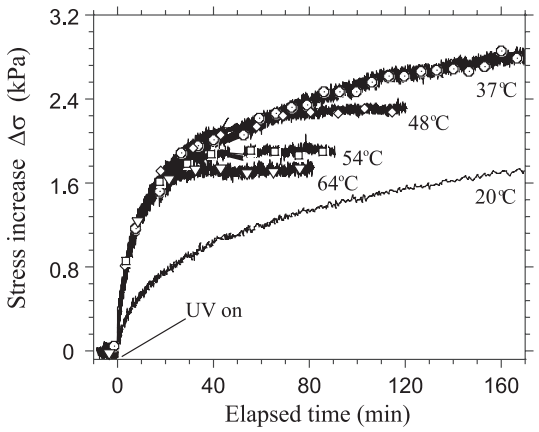

Fig. 6. The stress increase $\Delta\sigma$ caused by the photo-induced *trans*→*cis* isomerisation. The initial temperatures for these experiments are 64.4, 54.3, 48.4, 37.4 and 20.9 °C, as labelled on the plot.

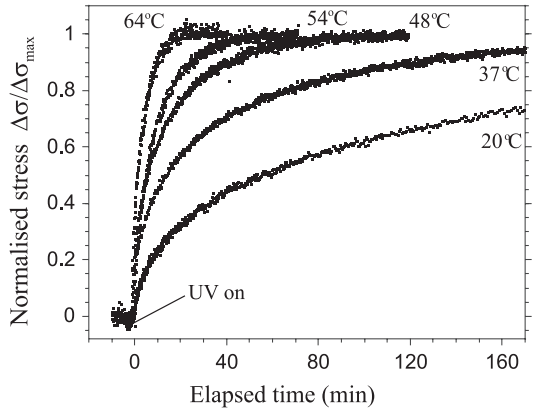

Fig. 7. The normalised stress increase $\Delta\sigma/\Delta\sigma_{\max}$ caused by the photo-induced *trans*→*cis* isomerisation. The initial temperatures 64.4, 54.3, 48.4, 37.4 and 20.9 °C are labelled on the plot.

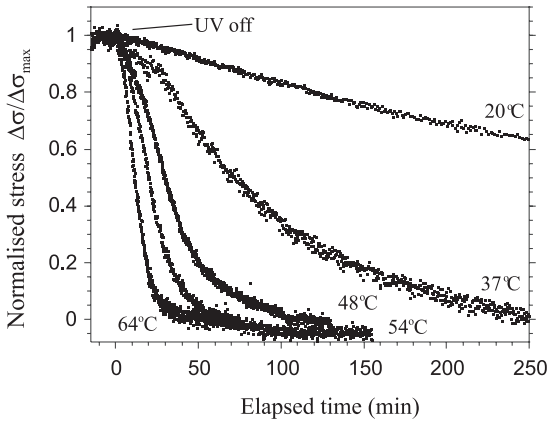

Fig. 8. The normalised stress decrease $\Delta\sigma/\Delta\sigma_{\max}$ due to the thermal *cis*→*trans* relaxation in the dark. The temperatures are the same as in Figures 6 and 7.

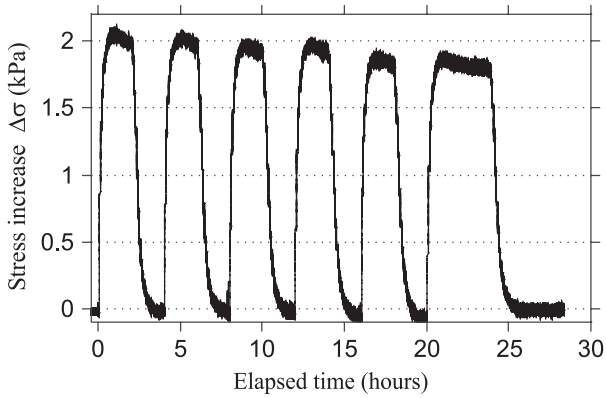

Fig. 9. Stress variations during several light/dark cycles, at a constant temperature of 56 °C.

UV, was heated by radiation[6], a slight temperature increase (of $\sim$ 0.5 °C) caused an additional force increase not related to the photo-isomerisation.

Thus, for more clarity, in the remaining of this paper we present the results corrected for these unwanted temperature variations. For the proper temperature adjustment one subtracts from the raw measured force the value it *would* have without the UV, at the current (increasing) temperature. To find the latter, we simply record, independently, the variation of force against temperature as in Figure 4(b).

The force responses were recorded at various initial temperatures and adjusted to the fixed value of temperature as described above. The amplitude of mechanical response depends on temperature, being steeper in the vicinity of $T_{\rm ni}$, see [2] for more details. Figure 6 shows the set of such stress increases at different temperatures. The overall magnitude of the effect is given by the saturation level $\Delta\sigma_{\max}$, the difference between the value the stress finally reached and its value before the UV to be switched on. The magnitude of $\Delta\sigma_{\max}$ varies over our range of temperatures, but remains in the range of 1.5–3.5 kPa. To specifically compare the rates of the response, we plot in Figures 7 and 8 the normalised results for the increase in stress $\Delta\sigma/\Delta\sigma_{\max}$ on irradiation, and the corresponding thermal relaxation of stress in the dark.

As the stress again reaches its initial value after the UV radiation is switched off, one could expect the effect to be repeatable. Figure 9 shows such a test of repeatability, a crucial characteristic if one is to have a practical application in mind. Overall, the effect is clearly reproducible, however, a small decay was found when repeating the light/dark cycle many times. We attribute this weakening to the destruction of few azobenzene groups (photo-bleaching), after several *trans*→*cis*→*trans* cycles (one must remember the equilibrium reached upon UV irradiation is dynamic, so that the molecules are continuously cycling from *cis* down to *trans* and back up again).

[6] This was checked by blocking the UV radiation in the setup remaining otherwise unchanged. In this case neither temperature nor force increase has occurred.

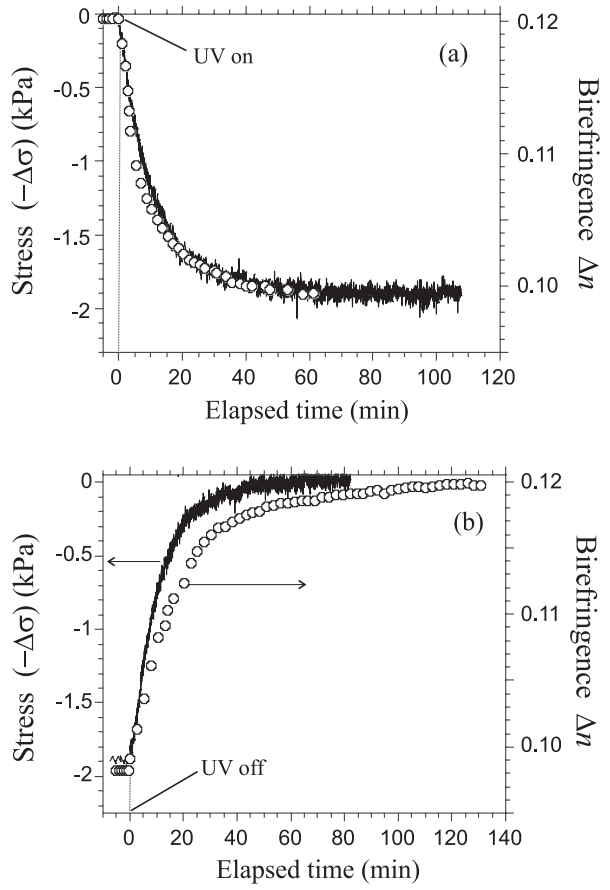

Fig. 10. Simultaneous plots of the stress (scatter line, left y-axes) and birefringence (open circles, right y-axes), changing when radiation is applied and then switched off. The birefringence decrease (increase) reflects the loss (recovery) of nematic order, which occurs with a rate close to the one of the mechanical response. The stress variations have been inverted to superpose the curves and show their similarities.

4 Order parameter and population dynamics

The linear population dynamics model presented here is derived from the one proposed in [2]. Despite the good agreement with experiment, one could argue that it is not the only possibility. And indeed, at this point, only the final predictions made in equations (6) and (7) were compared with experimental results. This dynamics could instead be explained in terms of a mechanical relaxation in the polymer network, the times measured being in fact those needed for the polymer chains to respond. So, it was crucial to check experimentally the main ideas expressed in the simple analysis of isomerisation dynamics.

An answer, albeit qualitative, is given by Figure 10, in which both the birefringence and the stress variations (Δn and the negative of $\Delta\sigma$, respectively) are plotted. The stress variation has been inverted (we actually plot $\sigma_{\text{initial}} - \sigma(t)$) for an illustrating purpose, to superpose both data sets and show they have *the same* characteristic dynamics. We do not say the relaxation times are equal, but they clearly are of the same order of magnitude. This result is important. First of all, it proves the nematic order (closely reflected by Δn) actually diminishes upon UV irradiation. Secondly, it shows that this order decreases and then increases with a speed roughly as the stress variations, and is therefore the rate-limiting process in this photo-actuation.

As explained in the Introduction, the proportion of *cis* isomers influences the macroscopic shape of the elastomer through the decrease in the nematic order parameter Q. The photo-isomerization of small-molecular-weight azobenzene compounds, in solution, is known to follow simple first-order kinetics. Only minor modifications were found when the reaction occurs in a dense polymer matrix [13]. We will therefore assume, as was done in references [1,2], that the population dynamics is first order, and more precisely described by equation

$$\frac{\partial}{\partial t} n(t,T) = -\eta\, n - \frac{1}{\tau_{tc}} n + \frac{1}{\tau_{ct}} (n_0 - n)\,, \qquad (2)$$

where n denotes the number of *trans* azobenzene moieties, n_0 the total number of *trans* plus *cis* isomers (which is constant and given by the initial composition, Fig. 2). τ_{tc} and τ_{ct} are the characteristic times of spontaneous *trans*→*cis* and *cis*→*trans* transformations, respectively. Unlike the *cis*→*trans* transition, the *trans*→*cis* process does not occur spontaneously on heating. Accordingly, we shall neglect τ_{tc} compared with τ_{ct}. The forced UV isomerisation occurs with the rate $\eta \equiv 1/\tau_{uv} \propto$ the radiation intensity.

One can easily obtain the number of *cis* isomers upon irradiation

$$n_{cis}(t) = n_0\,(1 - \tau_{\text{eff}}/\tau_{ct}) \left(1 - \exp^{-t/\tau_{\text{eff}}}\right)\,, \qquad (3)$$

where the light is switched on at $t = 0$ and the notation

$$\tau_{\text{eff}} = \frac{1}{\eta + 1/\tau_{ct}} = \frac{\tau_{ct}}{1 + \eta\tau_{ct}}$$

is used. Setting η to 0, and assuming in equation (3) that $n_{cis} = n_{cis}(\infty)$ (that is, that the saturation is reached on irradiation, which is the case experimentally), the relaxation dynamic is given by

$$n_{cis}(t) = -n_{cis}(\infty) \exp^{-t/\tau_{ct}} \qquad (4)$$

where the light is switched off at $t = 0$.

And now, how to take into account the destabilising effect of the contorted *cis* isomers? As was done in [2], we shall simply consider them as impurities shifting the critical temperature of the nematic-isotropic transition. Thus, as the mechanical properties of the elastomer are depending on $T - T_{\text{ni}}$, this is equivalent to shifting the actual temperature of the material. We will assume this shift to be linear, equation (5). This approximation is justified by the rather small value of the factor (in front of $T - T_{\text{ni}}$) this shift will be found to equal. This factor β is positive: the impurities weaken the order of the nematic liquid crystal:

$$T_{\text{eff}} = T_{\text{measured}} + \beta\, n_{cis}\,. \qquad (5)$$

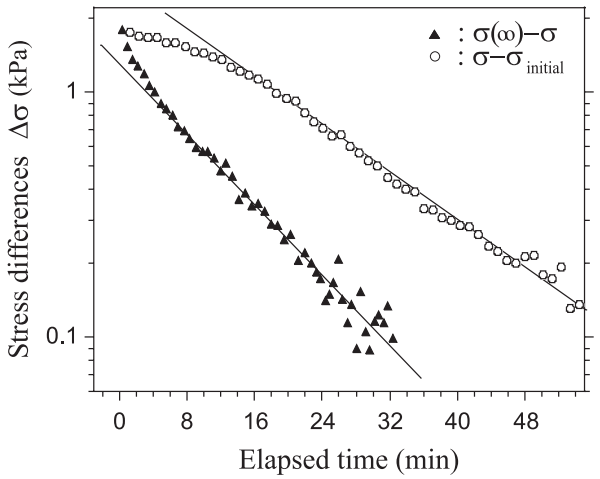

Fig. 11. The stress variations with (▲) and without (○) UV, in a log-linear scale. The straight lines correspond to the theoretical predictions of the linear relaxation model, see text. The isomerisation times thus obtained are plotted in Figure 12.

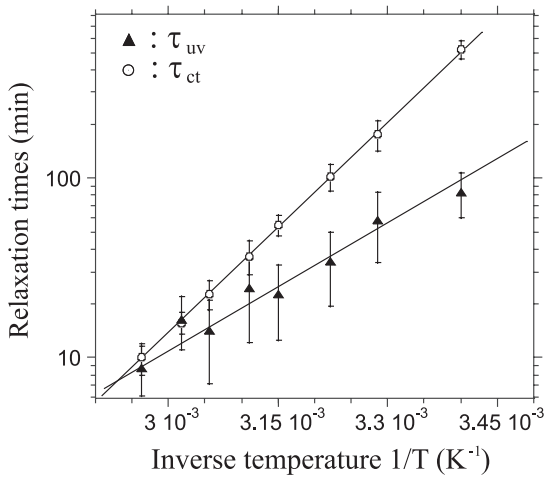

Fig. 12. The characteristic times, τ_{uv} (▲) and τ_{ct} (○) obtained from the linear relaxation model fitting; the straight lines are fitting the data, assuming an Arrhenius behaviour ($\tau \propto \exp(E_a/k_{\mathrm{B}}T)$).

The experimentally measured relation between stress and temperature, an example of which is given by Figure 4(b), can then be used to obtain the stress variation generated by this effective temperature shift. The stress-temperature relation, over the whole range of available temperatures, is of course highly non-linear. However, again, as the relative effective temperature shift, or the relative stress increase, are small in our experiments, one can approximate it as a linear function around each particular experimental temperature. So, finally, the following relation stands for the measured stress under irradiation

$$\sigma(t) - \sigma_{\mathrm{initial}} = \Delta\sigma_{\max}\left(1 - \exp^{-t/\tau_{\mathrm{eff}}}\right) \qquad (6)$$

while the relaxation is described by

$$\sigma(t) - \sigma_{\mathrm{initial}} = \Delta\sigma_{\max}\exp^{-t/\tau_{ct}} \qquad (7)$$

with

$$\Delta\sigma_{\max} = a\,\beta n_0\,(1 - \tau_{\mathrm{eff}}/\tau_{ct})\,,$$

a being the slope of the discussed linear stress-temperature relation (which can be easily obtained experimentally) at the temperature of irradiation. $\sigma_{\mathrm{initial}}$ is the stress set at the beginning of the experiment, before any UV to be applied (equal in our case to 21.7 kPa for all measurements).

Does this rather simple model fit our results? $\Delta\sigma_{\max}$ is directly obtained by subtracting the initial stress $\sigma_{\mathrm{initial}}$ from the steady-state saturation value reached under irradiation. Then, only one free parameter remains: the characteristic time, τ_{eff} for the excitation and τ_{ct} for the relaxation. An example is given for both excitation and relaxation in the log-linear plots in Figure 11. If equations (6) and (7) are correct then these curves should be linear. This appears to be true, except for very short times where one can notice, respectively, anomalously fast (at the beginning of the forced excitation) and slow responses (at the beginning of the thermal relaxation). This small deviation from the linear model could be caused by a slightly more complicated isomerisation kinetics, perhaps dependent on a less trivial shape of the energy barrier separating the isomer states. But it is not caused by the actual non-linearity of the stress-temperature relation, Figure 4(b), for explicitly taking into account this non-linearity does not improve the data fits at all. Whatever the physical reason, the correction at short times is small and does not challenge the overall hypothesis of linear dynamics.

Fitting the time dependence of the stress increase on irradiation, or the decrease on thermal relaxation, provides values of τ_{eff} and τ_{ct} at different temperatures, and thus the value of the isomerisation rate

$$\tau_{uv} \equiv \frac{1}{\eta} = \frac{1}{1/\tau_{\mathrm{eff}} - 1/\tau_{ct}}.$$

Figure 12 is an Arrhenius plot of these characteristic times enabling us to estimate the energy barriers for the isomerisation. We find $E_a = 0.5$ eV for the light-induced *trans* to *cis* reaction (τ_{uv}) and $E_a = 0.77$ eV for the spontaneous thermal relaxation (τ_{ct}). These times and activation energies are of the same order of magnitude as those obtained by Eisenbach [13] when studying the population dynamics of photo-isomerisable azobenzene compounds in an ordinary isotropic polymer matrix. In the framework of this model, we can also calculate the factor

$$\beta n_0 = \frac{\Delta\sigma_{\max}}{a\,(1 - \tau_{\mathrm{eff}}/\tau_{ct})},$$

as all the terms on the right-hand side are accessible experimentally. This product, reflecting the ultimate efficiency of the material as a transducer (assuming $\tau_{\mathrm{eff}}/\tau_{ct} \gg 1$), is equal to 4.0 ± 1 °C, which is very close to the value found in [2] by a different method.

Conclusion

In this work, we have explored the response of a novel photo-mechanical transducer generating the deformations

of forces many orders of magnitude higher than the effects known before. The explanations given to the phenomenon, based on the direct effect of photo-isomerisation on the nematic order parameter and that on the mechanical state of nematic rubber, have been accurately validated. We point out that the actuation speed is dominated by the photo-isomerisation dynamics, which appears to be very slow in a dense polymer matrix. On the one hand, the isomerisation rate η can be easily increased by simply using more intense radiation. On the other hand, even leaving aside adverse effects of photo-degradation, the overall magnitude of the response, reflected by the effective temperature shift, should be ultimately limited at βn_0 ($\simeq 4$ °C in our material).

For practical applications, as well as for a better understanding of the fundamental phenomenon, it would be very interesting to check these assertions, using various intensities of light. The maximum temperature shift obtained with our elastomer could seem small, but can however generate noticeable contractions or forces. Its intensity should be magnified in the vicinity of the critical temperature, because of the higher slope of the underlying thermo-mechanical behaviour there (see Fig. 4). It would therefore be useful to synthesise elastomers with transition temperatures close to the ambient 20 °C.

This research was made possible due to the Visiting Fellowship (Stage de Maîtrise) of JC, provided by the École Normale Supérieure de Cachan. We thank EPSRC UK for the support of ART. Invaluable experimental help of Sébastien Courty, Laurent Costier, Atsushi Hotta and Richard Gymer is gratefully appreciated, as are the discussions with Mark Warner and Yong Mao.

References

1. H. Finkelmann, E. Nishikawa, G.G. Pereira, M. Warner, Phys. Rev. Lett. **87**, 015501 (2001).
2. P.M. Hogan, A.R. Tajbakhsh, E.M. Terentjev, Phys. Rev. E **65**, 041720 (2002).
3. H. Finkelmann, H.J. Koch, G. Rehage, Macromol. Rapid Commun. **2**, 317 (1981).
4. J. Küpfer, H. Finkelmann, Macromol. Chem. Rapid Commun. **12**, 717 (1991).
5. M. Hébert, R. Kant, P.-G. de Gennes, J. Phys. I **7**, 909 (1997).
6. H. Wermter, H. Finkelmann, *e-Polymers* (`www.e-polymers.org`) no. 013 (2001).
7. A.R. Tajbakhsh, E.M. Terentjev, Eur. Phys. J. E **6**, 181 (2001).
8. M. Warner, K.P. Gelling, T.A. Vilgis, J. Chem. Phys. **88**, 4008 (1988).
9. S.S. Abramchuk, I.A. Nyrkova, A.R. Khokhlov, Polym. Sci. USSR **31**, 1936 (1989).
10. D.H. Waldeck, Chem. Rev. **91**, 415 (1991).
11. N.R. King, E.A. Whale, F.J. Davis, A. Gilbert, G.R. Mitchell, J. Mater. Chem. **7**, 625 (1997).
12. J.L.R. Williams, R.C. Daly, Prog. Polym. Sci. **5**, 61 (1977).
13. C.D. Eisenbach, Makromol. Chem. **179**, 2489 (1978).
14. M.-H. Li, P. Auroy, P. Keller, Liq. Cryst. **27**, 1497 (2000).
15. O. Tsutsumi, T. Shiono, T. Ikeda, G. Galli, J. Phys. Chem. B **101**, 1332 (1997).
16. L. Matějka, M. Ilavský, K. Dušek, O. Wichterle, Polymer **22**, 1511 (1982).
17. C.D. Eisenbach, Polymer **21**, 1175 (1980).
18. S.M. Clarke, E.M. Terentjev, Phys. Rev. Lett. **81**, 4436 (1998).
19. A. Hotta, E.M. Terentjev, J. Phys. C **13**, 11453 (2001).
20. A. Shishido, O. Tsutsumi, T. Ikeda, Mater. Res. Soc. Symp. Proc. **425**, 213 (1993).
21. J. Küpfer, H. Finkelmann, Macromol. Rapid Commun. **12**, 717 (1991).
22. N. Boden, R.J. Bushby, L.D. Clark, J. Chem. Soc., Perkin Trans. **1**, 543 (1983).
23. A.I. Vogel, *Vogel's Textbook of Practical Organic Chemistry*, 5th edition (Wiley & Sons, New York, 1989) p. 957.
24. S.K. Prasad, G.G. Nair, Adv. Mater. **13**, 40 (2001); P. Vanoppen, P.C.M. Grim, M. Rücker, S. De Feyter, G. Mössner, S. Valiyaveettil, K. Müllen, F.C. De Schryver, J. Phys. Chem. **100**, 19636 (1996).
25. H. Finkelmann, H.J. Koch, W. Gleiss, G. Rehage, Macromol. Chem. Rapid Commun. **5**, 287 (1984); G.R. Mitchell, M. Coulter, F.J. Davis, W. Guo, J. Phys. II **2**, 1121 (1992).
26. K. Lim, J. Ho, Mol. Cryst. Liq. Cryst. **47**, 173 (1978).